Atmos. Chem. Phys. Discuss., 13, 24635–24674, 2013
www.atmos-chem-phys-discuss.net/13/24635/2013/
doi:10.5194/acpd-13-24635-2013

Atmospheric Chemistry and Physics Discussions

A case study into the measurement of ship emissions from plume intercepts of the NOAA Ship *Miller Freeman*

C. D. Cappa[1], E. J. Williams[2,3], D. A. Lack[2,3], G. M. Buffaloe[1], D. Coffman[7], K. L. Hayden[5], S. C. Herndon[4], B. M. Lerner[2,3], S-M. Li[5], P. Massoli[4], R. McLaren[6], I. Nuaaman[5,6], T. B. Onasch[4], and P. K. Quinn[7]

[1]Department of Civil and Environmental Engineering, University of California, Davis, California 95616, USA
[2]NOAA Earth System Research Laboratory, Boulder, CO, 80305, USA
[3]Cooperative Institute for Research in Environmental Sciences, University of Colorado, Boulder, Colorado, 80305, USA
[4]Aerodyne Research, Inc., Billerica, Massachusetts, 01821, USA
[5]Air Quality Research Division, Environment Canada, 4905 Dufferin St., Toronto, M3H5T4, Canada
[6]Centre for Atmospheric Chemistry, York University, 4700 Keele St., Toronto, M3J1P3, Canada
[7]NOAA Pacific Marine Environment Laboratory, Seattle, Washington, 98115, USA

Received: 15 August 2013 – Accepted: 31 August 2013 – Published: 23 September 2013

Correspondence to: C. D. Cappa (cdcappa@ucdavis.edu)

Published by Copernicus Publications on behalf of the European Geosciences Union.

ACPD
13, 24635–24674, 2013

Abstract

Emissions factors (EFs) for gas and sub-micron particle-phase species were measured in intercepted plumes as a function of vessel speed from an underway research vessel, the NOAA Ship *Miller Freeman*, operating a medium-speed diesel engine on low-sulfur marine gas oil. For many of the particle-phase species, EFs were determined using multiple measurement methodologies, allowing for an assessment of how well EFs from different techniques agree. The total sub-micron PM (PM_1) was dominated by particulate black carbon (BC) and particulate organic matter (POM), with an average POM / BC ratio of 1.3. Consideration of the POM / BC ratios observed here with literature studies suggests that laboratory and in-stack measurement methods may overestimate primary POM EFs relative to those observed in emitted plumes. Comparison of four different methods for black carbon measurement indicates that careful attention must be paid to instrument limitations and biases when assessing EF_{BC}. Particulate sulfate (SO_4^{2-}) EFs were extremely small and the particles emitted by *Miller Freeman* were inefficient as cloud condensation nuclei (CCN), even at high super saturations, consistent with the use of very low sulfur fuel and the overall small emitted particle sizes. All measurement methodologies consistently demonstrate that the measured EFs (fuel mass basis) for PM_1 mass, BC and POM decreased as the ship slowed. Particle number EFs were approximately constant across the speed change, with a shift towards smaller particles being emitted at slower speeds. Emissions factors for gas-phase CO and formaldehyde (HCHO) both increased as the vessel slowed, while EFs for NO_x decreased and SO_2 EFs were approximately constant.

1 Introduction

Emissions of particulate matter (PM) and trace gases from ships operating in the open ocean as well as in coastal and inland waterway areas have significant impacts on air quality and climate (Corbett et al., 2007; Fuglestvedt et al., 2009). Quantification of

ACPD
13, 24635–24674, 2013

these impacts requires use of detailed emissions inventories and the specification of emission factors (EFs) to determine the spatial distribution of emissions. Emission factors for ships are commonly determined from (i) direct stack sampling of in-use ships, (ii) interception of emitted plumes from in use ships or (iii) from test engines in laboratories. Various studies indicate that EFs for total PM and different PM species can be highly variable between different ships. This variability reflects real differences in ship operation and the resulting emissions, but may also reflect differences between the measurement or sampling methodologies employed between different studies. Detailed characterization of the emissions from a single ship using multiple measurement techniques for a given species can facilitate understanding of the role that methodological differences play in determining measured EFs.

In addition, changes in engine load, which often correspond to changes in vessel speed, are known (Lloyd's Register Engineering Services, 1995) to have a large influence on the overall efficiency of the combustion process, with fuel economy (F_{econ}; e.g. km kg-fuel^{-1}) often increasing with decreasing speed and engine load. This increase in fuel efficiency generally translates to a decrease in emissions for a given pollutant, however the magnitude of the change is modified by the specific response of the emission factor for that pollutant to the change in speed (Lack et al., 2011). Such efficiency gains have motivated consideration and implementation of speed restrictions (or a fuel tax aimed at speed reduction) near some coastal and port regions or along shipping routes (Corbett et al., 2009; Buhaug et al., 2009). Most such efforts are aimed at decreasing emissions from large ocean going vessels. However, the operation of smaller crafts near coastal regions and inland waterways also contributes to local pollution (Corbett and Fischbeck, 2000), and thus the dependence of their emissions on vessel speed must also be understood so that appropriate pollution control strategies in those regions can be developed. This is particularly the case for smaller vessels that are likely to operate at speeds and engine loads that are more variable than large ocean going vessels. Furthermore, vessels that operate in shorter time-frame service operations near coastal environments have highly variable load distributions and ages,

ACPD
13, 24635–24674, 2013

and thus it is necessary to characterize emissions factors and their speed dependence for both newer and older vessels. Development of next-generation emissions inventories will result from such higher resolution assessments of the dependence of and variations in engine load distributions, fleet age and emission factor with engine load, engine age and vessel speed (Wang and Minjares, 2013).

Here, we report measurements of both PM and gas-phase EF values for a series of plumes emitted by the NOAA Ship *Miller Freeman*, which was in transit within regulated waters off the coast of Santa Barbara, CA and intercepted during the 2010 CalNex field campaign (Ryerson et al., 2013). Regulated waters correspond to the region within 24 nautical miles of the CA baseline where, as of 1 July 2009, ocean going vessels were required to utilize fuels with ≤ 1.5 % sulfur (California Air Resources Board, 2011). (The fuel sulfur requirement has since been reduced to ≤ 1 %, as of August 2012 and will further decrease to ≤ 0.1 % in 2014.) The PM measurements were made using a suite of different measurement techniques, some of which overlap in terms of the specific PM species measured. In addition, the intercepted plumes were emitted while the *Miller Freeman* operated at 4 different but constant speeds, and thus enables an assessment of the influence of vessel speed on the emissions from vessels of this type. The *Miller Freeman* is a 65.5 m (215 ft) fisheries and oceanographic research vessel with a cruising speed of 11 knots, running a single 1.64 MW geared medium-speed diesel (MSD) main engine from General Electric with a rated power of 2.2 khp and with a controllable pitch propeller (NOAA, 2010). The *Miller Freeman* is an older vessel, launched in 1967, that was decommissioned in 2013. During the plume intercepts the *Miller Freeman* was operating on a mix of, "ultra-low sulfur diesel from California mixed with standard marine diesel from Washington [state]" (Field Operations Officer, personal communication, 2010.). Fuel samples were not available for off-line analyses, but as we show later the fuel sulfur content is estimated to be around 0.1 % by weight, consistent with marine gas oil (MGO) or marine distillate oil (MDO) fuels, which will be referred to generically as low sulfur fuels (LSF).

ACPD
13, 24635–24674, 2013

The measurements reported here therefore provide a case study allowing for assessment of how well different measurement techniques agree in terms of the derived EFs and for the influence of vessel speed on older, smaller MSD vessels operating on LSF, which are an important class of vessels that operate in near-coastal and inland waterways. For example, plumes were encountered for a number of other MSD vessels with build years ranging from 1952 to 2006 during CalNex, with most of these being pre-1990 vessels. This is generally consistent with the average age (as of 2010) of "other" vessels (i.e. exclusive of container, bulk, cargo and tanker vessels) in the world merchant fleet being 25 yr (United Nations Conference on Trade and Development, 2011) and with 43 % of such vessels (i.e. passenger, offshore, service and tugs) in 2011 being older than 25 yr (Equasis, 2012). Further, larger ocean going vessels are increasingly having to switch to LSFs from the commonly used high-sulfur heavy fuel oil (HFO, or bunker fuel) during operation near coasts (US EPA, 2010; California Air Resources Board, 2011). (Although there were plumes from many other ships intercepted during CalNex, not all instruments were operating at all times under conditions that allow for determination of EFs, and thus we restrict this study to the ship for which the most comprehensive measurements are available.) The results here are compared with literature results from test rig, in-stack and plume studies to place them in the broader context that is necessary for development of next-generation emissions inventories.

2 Experimental

Emissions factors for PM and trace gases (CO, SO_2, HCHO and NO_x) were measured using the plume intercept method (also known as the "sniffer" method), wherein concentrations of the pollutants are measured in a plume that is intercepted downwind of the vessel of interest, here the *Miller Freeman*. One benefit of the plume intercept method is that atmospherically relevant dilution factors and temperatures are achieved by the time the plume is sampled, although the exact extent of dilution varies

ACPD
13, 24635–24674, 2013

for each plume and the plume must be identifiable above background concentrations. Gas-phase and PM measurements were made onboard the NOAA-sponsored Woods Hole R/V *Atlantis* as part of the CalNex field campaign (Ryerson et al., 2013). The emissions plume from *Miller Freeman* was intercepted on five occasions on May 19, 2010, with *Miller Freeman* traveling at four different speeds: 2.9 knots, 6.9 knots (twice), 10.2 knots and 12 knots. The coordinated effort between the ships allowed for measurements to be made in plumes that were emitted when *Miller Freeman* was traveling at a constant speed. Plumes from *Miller Freeman* were identified by combining the relative ship positions with the local wind direction and wind speed data measured from *Atlantis*. Using these data, local back trajectories from *Atlantis* were computed by simple vector analysis to determine the location of and speed at which *Miller Freeman* was cruising at the time the pollutants were emitted and to estimate the age of each plume encountered. Separation distances between the ships were from 200 to 900 meters; plume travel times were from 1 to 5 min (Table 1). Engine load (F_{load}) information is not directly available from the *Miller Freeman*. For marine vessels engine load is often estimated from the vessel speed (u) using a cubic power law relationship (the so-called propeller law), where $F_{load} = (u_{actual}/u_{max})^3$ (Corbett et al., 2009). However, because the *Miller Freeman* operated a controllable pitch propeller, as opposed to a fixed pitch propeller, the power law is likely not appropriate. Nonetheless, estimated engine load values from the propeller law are reported here for reference. We assume that the maximum speed encountered here, 12 knots, corresponds to u_{max}; the F_{load} values are then 1.4 %, 19 %, 61 % and 100 %, respectively. This lowest F_{load} value is lower than typical values under idling conditions, indicating a likely failure of the propeller law for this vessel. The encounter occurred during late afternoon when the temperature was between 11.9 °C and 12.2 °C and the relative humidity was between 88 % and 93 % (although particles were dried before sampling).

Gas-phase measurements included CO_2, NO_x, CO, SO_2 and HCHO with uncertainties of ±0.25 ppmv, ±20 %, ±4.1 % and ±15 % and ±9 % (Williams et al., 2009). Particle phase instrumentation included an Aerodyne high-resolution time-of-flight aerosol

ACPD
13, 24635–24674, 2013

mass spectrometer (HR-AMS) for measurement of particulate SO_4^{2-}, NO_3^-, NH_4^+, Cl^- and OM (Canagaratna et al., 2007), a Droplet Measurement Technologies single particle soot photometer (SP2) for refractory BC (rBC) particle mass and number concentrations and size distributions (Schwarz et al., 2006), an Aerodyne Soot-Particle AMS (SP-AMS) for refractory BC particle mass and OM and SO_4^{2-}, NO_3^-, NH_4^+ and Cl^- rBC coating mass concentrations (Onasch et al., 2012), TSI 3025A (CN > 3 nm) and 3010 (CN > 12 nm) condensation particle counters for particle number concentrations, a cloud condensation nuclei (CCN) counter (DMT, Inc.) (Roberts and Nenes, 2005), a photo-acoustic spectrometer (PAS, operating at 532 nm and 405 nm) for light absorption (Lack et al., 2012), one three-wavelength particle soot absorption photometer (PSAP, at 450, 530 and 700 nm) for light absorption (Virkkula et al., 2005), a cavity ring-down spectrometer (CRD, at 532 nm) for light extinction and optical hygroscopicity measurements (Langridge et al., 2011) and a scanning mobility particle sizer (SMPS, TSI, Inc.) for particle size distribution measurement operating with a scan time of 2.5 min . For the HR-AMS, a collection efficiency (CE) of 1.0 has been assumed; this means that the EFs determined from this instrument are lower limits. While the CE for HR-AMS is mostly caused by particle bounce on the vaporizer (Huffman et al., 2005; Matthew et al., 2008), the CE in the SP-AMS is primarily a function of the degree of overlap between the particle and laser beams and the laser power profile in the overlapping region (Onasch et al., 2012). For the SP-AMS, a CE for BC of 0.2 ± 40 % is used while a CE = 0.4 ± 100 % is used for non-BC components that are internally mixed with BC (see Supplement). Note that the precision of the measusred BC and non-BC species concentrations is substantially better than the above uncertainties indicate, which account for measurement accuracy. The SP2 was calibrated using fullerene soot particles, which have been shown to give a similar response as diesel soot (Laborde et al., 2012). The SP2 measured particles with volume equivalent diameters ($d_{p,VED}$) between 60 nm and 300 nm. The SP2 rBC concentrations were corrected for the measured particle detection efficiency of 0.7 for particles with $d_{p,VED} > 100$ nm. For $d_{p,VED} \leq 100$ nm, a size-dependent detection efficiency was applied to the data to account for the fall off

ACPD
13, 24635–24674, 2013

in instrument sensitivity (see Supplement; Schwarz et al., 2010; Liggio et al., 2012). Overall uncertainties for the particle measurement instrumentation are estimated to be +35 %/−15 % (HR-AMS), +100/−20 % (SP2), ±40 % (SP-AMS, BC), ±100 % (SP-AMS; non-BC), ±5 % (CN), ±10 % (CCN), ±7 % (PAS, 532 nm), ±15 % (PAS, 405 nm), ±20 % (PSAP) and ±1 % (CRD), when signals are well above their detection limits. Plume-specific detection limits, given as DL = $3\sigma/\sqrt{N}$, were assessed, where σ is the standard deviation observed during the background periods just before/after the plume and N is the number of data points across an individual plume. Typical values of N were around 70 points per plume, except for CCN (see Supplement). Absolute EF values are only reported when the in-plume signals were above the detection limit.

Particle-phase EFs were determined using an area-ratio approach, where the background-subtracted area under the ship plume (i.e. plotted as concentration vs. time) for the pollutant of interest is divided by the similarly-calculated area under the CO_2 plume. The ratio gives the EF after appropriate unit conversion and multiplication by the mass fraction of carbon in the fuel, which was assumed to be 0.865 (Lack et al., 2009; Williams et al., 2009). Specifically,

$$\mathrm{EFX} = \frac{A_{\mathrm{X,bgd}}}{A_{\mathrm{CO_2,bgd}}} \cdot f_{\mathrm{fuel}} \quad (1)$$

where $A_{\mathrm{X,bgd}}$ is the background-subtracted concentration of species X, integrated over the entire plume, $A_{\mathrm{CO_2}}$,bgd is the same for CO_2 and f_{fuel} is the conversion factor between CO_2 (in ppmv) and fuel consumed (kg-fuel). The area-ratio approach is independent of the time-resolution of the instrumentation (which differs between different instruments) and has been used in other studies for calculating emission ratios of ship emissions (McLaren et al., 2012). Importantly, in the plume intercept method dilution is naturally accounted for because the pollutant of interest is ratioed to CO_2 concentrations, and CO_2 is non-reactive within the plume. Gas-phase EFs were determined using linear regression analysis since the time-resolution of all gas-phase instruments was identical and the area-ratio and linear regression methods give nearly identical

ACPD
13, 24635–24674, 2013

results (Williams et al., 2009). Although fuel carbon is also emitted as CO, combustion related hydrocarbons and particulate carbon, the majority of carbon is emitted as CO_2 (> 99 %, based on the derived EFs), and thus the determination of the various EFs using only CO_2 will lead to negligible biases. Given our method of determination, the EFs reported are related to the mass of fuel consumed, with units of emissions of X per kg of fuel (where emissions of X can be in grams, particles, etc.).

Conversion of the optical property measurements to mass EFs requires specification of the mass absorption or mass extinction efficiency (MAE or MEE). Specifically, division of the measured extinction coefficient by the MEE yields the mass concentration of PM_1, while division of the measured absorption coefficient by the MAE yields the mass concentration of equivalent black carbon (eBC; Petzold et al., 2013). Here, we use MAE = $10.2\,m^2\,g^{-1}$ (405 nm), $9.2\,m^2\,g^{-1}$ (450 nm), $7.75\,m^2\,g^{-1}$ (532 nm), $7.5\,m^2\,g^{-1}$ (550 nm) and $5.9\,m^2\,g^{-1}$ (700 nm), and MEE = $4\,m^2\,g^{-1}$ (532 nm). The MAE values were specified based on that reported by Bond and Bergstrom (2006) at 550 nm and extrapolated to other wavelengths assuming a $1/\lambda$ dependence. The MEE values are from Hand and Malm (2007). The uncertainty in the conversion for MAE is $\sim \pm 15$ %, while for MEE it is estimated as at least ±30 % based on the difference in the MEE between different particle components. Final uncertainties in the EFs were determined for each encounter for each instrument as the larger of the instrument uncertainty or the propagated standard deviation measured during the background (non-plume) period around each plume.

ACPD
13, 24635–24674, 2013

3 Results and discussion

3.1 Particle phase emissions

3.1.1 Mass emission factors

Emissions factors determined for all PM species that were measured are reported in Table 1 and shown in Fig. 1. The results are provided for each of the 5 plumes that were intercepted, which correspond to different vessel speeds at time of emission. The EF for PM_1 mass was determined either as the uncertainty-weighted sum of the chemically-specific measurements that were above detection limits (i.e. $EF_{PM_1,Sum} = EF_{BC} + EF_{POM}$, where EF_{SO_4} has been excluded because it is below the detection limit for all intercepts) or from the measurement of total light extinction ($EF_{PM_1,Ext}$). Overall, the two methodologies agree within uncertainties for each intercept, although for the three slowest speed intercepts the $EF_{PM_1,Sum} < EF_{PM_1,Ext}$ with the opposite true for the two highest speed intercepts. This may reflect speed-dependent variations in the POM / BC ratio (discussed further below), which can influence the MEE used to convert light extinction to PM_1 mass. On average, the two methods agreed to within 18 %. It is also evident that the EF_{PM_1} increases substantially with vessel speed (Fig. 1).

The EF_{PM_1} is dominated by contributions from POM and BC, with all other measured species, in particular SO_4^{2-}, contributing negligibly (Fig. 1). The EF for POM was determined from two independent instruments, the HR-AMS and the SP-AMS. Both methods determine POM concentrations via mass spectrometry, but they differ in their specific operation and, importantly, the SP-AMS as operated during CalNex was only sensitive to POM that existed in BC-containing particles while the HR-AMS measures POM in all particles. The two methods are highly consistent in their general dependence on vessel speed (Fig. 1), and the measured EF_{POM} values agreed on average to within 16 % despite the substantial uncertainty on the SP-AMS EF_{POM}. This consistency in behavior between the HR-AMS and SP-AMS with vessel speed suggests that a substantial fraction of the emitted POM mass is associated (i.e. internally mixed) with BC. The av-

ACPD
13, 24635–24674, 2013

erage EF_{POM} (0.39 ± 0.44 g kg^{-1} fuel) across all engine speeds is somewhat less than the multi-ship MSD average (0.65 ± 0.44 g kg^{-1} fuel) from Lack et al. (2009), although it is important to note that nearly all of the MSD vessels sampled by Lack et al. were tug boats, which likely have a different emissions profile than a research vessel such as the *Miller Freeman*. As with the EF_{PM_1}, the EF_{POM} increases with vessel speed.

The EF_{BC} was determined using four independent methods, two that measured equivalent BC (eBC) by light absorption measurement (PAS and PSAP), one that measured the laser induced incandescence by rBC-containing particles (SP2) and one that measured the rBC concentration via mass spectrometry (SP-AMS) (Petzold et al., 2013). There is good agreement in the EF_{BC} values determined between the two absorption based methods and the SP-AMS, while the SP2 gave systematically lower values. The good agreement of the PAS and PSAP derived EF_{BC} values indicates that positive biases that can be associated with PSAP measurements (Cappa et al., 2008; Lack et al., 2008a) are not significant for the plume particles, most likely because of the relatively large BC content. That the SP2-derived EF_{BC} is systematically lower than that determined using the other methods suggests that a substantial fraction of the BC mass exists in particles with volume equivalent diameters $d_{p,VED} < 60$ nm. This is addressed further in Sect. 3.1.4. This suggests that the SP2 may not be suitable for accurate determination of EF_{BC} for fresh ship emissions, although can provide a lower limit. The weighted average EF_{BC} (0.23 ± 0.15 g kg^{-1} fuel) across all engine speeds for *Miller Freeman* is on the low end of the multi-ship average (0.97 ± 0.66 g kg^{-1} fuel) determined by Lack et al. (2009) for vessels operating MSD engines. Again, this difference may reflect the difference between the *Miller Freeman* and the predominately tug boats sampled by Lack et al. (2009). As with the EF_{POM}, the EF_{BC} are observed to increase with vessel speed, although somewhat less steeply.

The EF_{SO_4} measurements from the HR-AMS and SP-AMS were below the detection limit at all speeds, and indicate that the SO_4 contribution to the total particle mass is small, consistent with the use of low sulfur fuel. EF_{SO_4} can also be estimated from the measured EF_{SO_2} (Sect. 3.2) based on previous results that indicate the percent

ACPD
13, 24635–24674, 2013

conversion of SO_2 to p-SO_4 in ship plumes from MSD vessels on the timescales considered here (a few minutes) is ~ 1–2 % (Lack et al., 2009). This yields EF_{SO_4} = 0.02–0.04 g kg^{-1} fuel, consistent with the directly measured EF_{SO_4} being below the plume-specific detection limits of the HR-AMS and SP-AMS (Table 1). As with p-SO_4^{2-}, EFs for particulate NO_3^-, NH_4^+ and Cl^- were at or below the detection limits.

3.1.2 The POM / BC ratio

The average particle composition calculated from the weighted average EF_{POM} and EF_{BC}, assuming only BC and POM contribute significantly to PM, is 53(±14) % POM and 47(±14) % BC, or POM / BC = 1.34 (±0.9) (Fig. 2). The uncertainty on the 2.9 knot plume is large. If this plume is excluded, the fraction of the PM_1 mass that is POM is observed to increase slightly as vessel speed increases, with POM / BC ranging from 0.6 (6.9 knots) to 3.0 (12 knots), with an average of 1.41. This is a result of the EF_{BC} increasing less steeply with ship speed than EF_{POM} (Fig. 1); this may be due to increased oil consumption at higher speeds. The average and range of POM/BC observed here are consistent with both the low-sulfur and the all-vessels plume intercepts results from Lack et al. (2009) (POM / BC = 0.8 and 1.48, respectively), the plume intercepts results from Lack et al. (2011) for the *Margrethe Maersk* (POM / BC = 1.3–2.6) and with two of the in-stack measurements: Jayaram et al. (2011) (POC / EC = 0.7–1.4) and Kasper et al. (2007) (POC / EC ~ 0.7–3). (We assume that POM / BC and POC / EC are sufficiently similar in magnitude such that they can be compared. Consider that the POM / POC ratio for ship emissions was measured to be ~ 1.2 (Murphy et al., 2009).) The POM / BC ratio observed here (and in the above cited studies) is, however, substantially smaller than all other in stack or test rig studies, including results reported by Petzold and co-workers for a test rig MSD operating on MGO (POM / EC = 3.6–8.7 and POM / BC = 6.9–77) (Petzold et al., 2011a) or heavy fuel oil (HFO) (POM / EC = 3.8–8.8 and POM / BC = 5.2–28) (Petzold et al., 2010), by Khan and co-workers for a slow speed diesel (SSD) (POC / EC = 50–74) (Khan et al., 2012a) and MSD (POC / EC =

ACPD
13, 24635–24674, 2013

3–15) (Khan et al., 2012b) vessel operating on MGO, by Agrawal and co-workers for a few SSD vessels operating on HFO (POC / EC = 8–33) (Agrawal et al., 2008a,b, 2010) or an auxiliary engine operating on MGO (POC / EC = 3–10) (Agrawal et al., 2008b). Murphy et al. (2009) report EFs from a single SSD vessel operating on HFO using both in stack and plume intercept methods and find values larger than those observed here, although with the in stack POC / EC (= 25) nearly twice as large as the plume intercept POM / BC (=13).

Plume intercept studies (this work; Lack et al., 2009, 2011; Murphy et al., 2009) measure the POM / BC ratio for emitted particles at atmospherically relevant dilutions while studies that utilize test-rigs or that sample directly from the ship stack will sample at varying dilution factors that depend on the exact methodology employed. Thus, one possible reason for the difference between our results and some of the literature could be that the results depend on the methodology used, with ambient methods (i.e. plume sampling) typically giving lower POM / BC than direct sampling (e.g. in stack) measurement methods, likely due to the relatively rapid dilution experienced by a plume a few minutes downwind of emissions (Petzold et al., 2008) and consequent evaporation of semi-volatile POM species. Evaporation of POM may be greater in plume intercept studies compared with direct sampling, depending on the level of dilution used during sampling and the resultant POM concentrations. This suggestion is consistent with observations that have shown the dilution ratio used during sampling from diesel engines can have a profound influence on the amount of organic carbon measured and the POC / EC ratio (Lipsky and Robinson, 2006; Fujitani et al., 2012). Consider also that Murphy et al. (2009) found the POM / BC from plume intercepts to be about half that of the POC / EC measured via in stack sampling for emissions from the same vessel. Given that EF_{BC} is independent of dilution (since BC is non-volatile) while EF_{OM} can be highly sensitive to dilution, our results, combined with literature results (e.g. Lack et al. (2009, 2011) and Murphy et al., 2009), indicate a potential for laboratory test rig and stack sampling methods to overestimate POM emission factors from ships and ship engines if sufficient dilution is not used during sampling. (It remains unclear why

ACPD
13, 24635–24674, 2013

the Jayaram et al. (2011) stack-sampling and Kasper et al. (2007) test rig studies give a similarly low POC / EC ratio.) Alternatively, it is possible that the difference between our LSF results and the literature studies that used HFO could result from typically greater use of lubricating oil with HFO, which could translate to greater emissions of POM. However, this does not seem likely because the ensemble results from Lack et al. (2009), which include vessels with a variety of ages and types, suggest relatively small differences in the POM / BC ratio between ships operating on LSFs vs. HFO or between different engine types.

We note that this discussion is limited to primary POM emissions; the loss of POM due to evaporation leads to the production of gas-phase organic matter, which can photochemically react in the atmosphere on timescales longer than the plume transit times encountered here to produce secondary POM. Thus, it may be that POM is only temporarily lost, although the likelihood of re-condensation is dependent upon a variety of parameters, such as the concentration of gas-phase oxidants, temperature, relative humidity, dilution, etc. In addition to evaporation considerations, there may be substantial differences (and large uncertainties) in the BC and EC measurements made using different techniques (Petzold et al., 2011b) that can also contribute to differences in reported POM / BC.

3.1.3 Particle number and size

Observed particle number concentration EFs (EF_{CN}) for the *Miller Freeman* varied from 1–3 × 10^{16} particles kg^{-1} fuel (Table 1). The average EF_{CN} for all particles with diameters > 3 nm were larger than for all particles with diameters > 12 nm (2.3(± 0.5)×10^{16} vs. 1.5(± 0.3) ×10^{16} particles kg^{-1} fuel, respectively). The EF_{CN} exhibited no particular dependence on vessel speed, both for $EF_{CN,>3\,nm}$ and $EF_{CN,>12\,nm}$ (Fig. 1).

It was possible to determine mobility diameter size distributions associated with the emitted particles for some of the plumes from the SMPS measurements (Fig. 3). This was not possible for all plumes (specifically, the two 6.9 knot plumes) because, due to

ACPD
13, 24635–24674, 2013

the narrowness of the plumes in time and the relative timing and long scan time of the SMPS, the plume-specific size distribution could not be resolved from the background (Fig. 3). The median number-weighted mobility diameter ($d_{p,m}$) measured did exhibit some dependence on vessel speed, increasing from ~30 nm at 2.9 knots, to 48 nm at 10 knots, to 69 nm at 12 knots. This observation is consistent with the observation that EF_{PM_1} increased with vessel speed while EF_{CN} was speed independent (Fig. 1).

In addition to mobility size distributions, the SP2 was used to determine volume equivalent diameter number and mass-weighted size distributions for the rBC component of the particles from 60 nm < $d_{p,VED}$ < 300 nm (the detection limits of this SP2). For non-spherical, fractal-like particles $d_{p,VED} < d_{p,m}$ (DeCarlo et al., 2004). The SP2 measures rBC size distributions with much higher time resolution than the SMPS making it possible to determine unique plume-specific size distributions for each intercept. The rBC number-weighted size distributions for the different plumes (Fig. 4) indicate that there is one mode that peaks at $d_{p,VED}$ ~100 nm and a second, much higher concentration mode that maximizes at some diameter <60 nm. (It is important to note that the exact shape of the distributions below 100 nm is highly dependent upon the size-dependent detection efficiency correction applied; see Supplement for further details.) This is consistent with the rBC number concentrations in the plumes, as measured by the SP2, being only ~1 % of the total CN and with the observation that most of the particles existed with $d_{p,m}$ < 100 nm (Fig. 3). This also provides a rationale for the systematically smaller EF_{BC} values from the SP2 compared to the other measurement techniques.

Particle coagulation can strongly influence the measured EF_{CN}, the extent to which depends both on how rapidly and by how much the sample is diluted. Plume intercept observations have shown there can be a rapid shift in the ratio between $EF_{CN,>5\ nm}$ and $EF_{CN,>10\ nm}$ with distance downwind of the target vessel (Lack et al., 2009; Petzold et al., 2008). For the plumes intercepted here there is some correspondence between the measured EF_{CN} and plume age, consistent with these previous observations and providing additional evidence that coagulation plays an important role in determining

ACPD
13, 24635–24674, 2013

the number concentration of particles in ship plumes. Given this, we suggest that the plume intercept method may be generally able to provide a more robust estimate of the absolute EF_{CN} most relevant to the atmosphere since it allows for determination of the EFs upon atmospherically relevant dilution factors and time-scales. However, in stack and test rig studies may allow for a more straightforward measure of the influence of operating parameters (e.g. fuel type, speed/engine load) on the EF_{CN} because they can be conducted at constant dilution factors.

Comparing with literature plume intercept studies, both the EF_{CN} and the peak sizes of the particle size distributions measured here are similar to that observed by Lack et al. (2011) 2.5–7.5 min downwind for an ocean going vessel operating an SSD on HFO or MGO ($EF_{CN,>4nm}$ = 1.0–1.4 × 10^{16} per kg fuel and $d_{p,m}$ = 65–35 nm). They also found that EF_{CN} was approximately constant while particle size increased with vessel speed for this vessel, although this occurred concurrent with a switch from operation on HFO to MGO making it difficult to separate fuel quality (i.e. sulfur content) from vessel speed effects. The EF_{CN} here are also similar to the average observed by Petzold et al. (2008) from an SSD vessel operating on HFO at 85 % of max power when plume age > 16 min ($EF_{CN,>1\,3nm}$ = 1.4 × 10^{16} per kg fuel). The *Miller Freeman* EF_{CN} are somewhat larger than the ensemble average measurements of Lack et al. (2009) for MSD and SSD vessels operating on either LSF and HFO ($EF_{CN,>5\ nm}$ = 1.25 × 10^{16} per kg fuel and $EF_{CN,>13\ nm}$ = 0.7 × 10^{16} per kg fuel). Petzold et al. (2008) also report one measured size distribution for which $d_{p,m} \sim 75$ nm, although they emphasized that the size distribution may rapidly shift as a plume is increasingly diluted downwind.

Considering in stack and test rig studies, Khan et al. (2012a) observed a very slight increase in $d_{p,m}$ with vessel speed at low speed ratios/loads for an SSD vessel operating on MGO. Kasper et al. (2007) observed a general, although not monotonic, increase in particle size with engine load for a SSD test rig operating on MDO, and that EF_{CN} was relatively constant for all F_{load} > 1 %. In contrast, Petzold et al. (2010), using HFO with an MSD test rig, observed a relatively continuous increase in EF_{CN} and decrease in particle size with engine load (although with some difference in EF_{CN}

ACPD
13, 24635–24674, 2013

at F_{load} = 100 % before/after the engine had warmed up). However, in a separate study Petzold et al. (2011a) observed that EF_{CN} decreased with test rig engine load for HFO operation, and that below F_{load} = 100 % the dependence of EF_{CN} on engine load was ambiguous for the same engine operating on various biofuels. Khan et al. (2012a) observed a strongly bimodal size distribution when a SSD vessel operated on HFO, but an approximately monomodal distribution when the same vessel operated on MGO. Additionally, they observed particle diameters were typically larger for HFO operation. Comparison of these various studies suggests that, in general, HFO operation tends to produce larger particles compared with LSF operation, consistent with the greater contribution of p-SO_4^{2-} to the total PM_1 mass when HFO is utilized.

3.1.4 Cloud condensation nuclei

The above discussion illustrates that fuel type plays a strong role in determining the emitted particle size distribution. Developing clearer understanding of the impacts of vessel operating parameters, such as fuel type or speed, on EF_{CN} and particle size is critical to understanding sources of new particles to the atmosphere, and their potential to ultimately act as cloud condensation nuclei (CCN). Understanding the size dependence of emitted particles is important because the emitted size will determine the probability that a given emitted particle will survive to grow into the CCN active size range (Pierce and Adams, 2007).

Direct measurements of the EF_{CCN} were made for all particles with aerodynamic diameters less than 1 µm at super saturations (SS) ranging from 0.3–0.7 %. The CCN instrument operated in a mode wherein the SS was varied with time, and thus the measurements are not consistent across all of the plumes encountered. This makes it difficult to generalize the relationship between CCN number and vessel speed from these measurements. The best coverage was obtained for total sub-micrometer particles when SS = 0.6 % and 0.7 %. The fraction of total CN that were CCN active at 0.6 % ranged from 0.004 to 0.007 and at 0.7 % ranged between 0.008–0.021 (see Table 1). These values are lower than those observed by Lack et al. (2009) at a lower

ACPD
13, 24635–24674, 2013

SS, 0.44 %, for a variety of vessels operating on higher sulfur fuel (CCN / CN = 0.42) or on fuel with < 0.5 % sulfur (CCN / CN = 0.07). They are also lower than observations at SS = 0.3 % for a single vessel as it operated on fuel with high sulfur content (~ 3 %; CCN / CN = 0.4), but are similar to observations for that same vessel operating on fuel with lower sulfur content (~ 0.2 %; CCN / CN = 0.007) (Lack et al., 2011); *Miller Freeman* was operating on fuel with sulfur content of ~ 0.1 % (see Sect. 3.2). It should be noted, however, that the higher SS used here should lead to overall higher CCN / CN, all other things being equal, which suggests that the CCN activity of the particles emitted by *Miller Freeman* was even lower than that observed by Lack et al. (2011) and is consistent with the p-SO_4^{2-} being a smaller fraction of the total PM in this study.

Our results indicate that directly emitted particles act inefficiently as CCN even at high super saturations (SS = 0.7 %). Additionally, there is less gas-phase sulfur emitted (Sect. 3.2) that could ultimately lead to downwind growth of the emitted particles. It is evident that the use of LSFs leads to substantially reduced emissions of both direct and potential CCN relative to higher sulfur fuels. As has been previously noted (Lauer et al., 2009; Lack et al., 2011), this reduction in CCN associated with shifts towards low sulfur fuels has substantial implications for the likelihood of ship track formation and the currently net cooling effect of PM emitted by ships – and thus for future regulation of the sulfur content of fuel used by ships. However, this climate impact must be balanced with the net benefits to air quality that derive from reductions in the emitted PM (Arneth et al., 2009). It is also important to note that since the low sulfur fuel in use by *Miller Freeman* had a sulfur content of only ~ 0.1 % these results are most applicable to vessels operating in sulfur emissions control areas in near shore environments around California or the North and Baltic Seas. Sulfur content for fuels in use by vessels on the high seas is currently limited by the IMO only to 3.5 %, and it has been suggested that this fuel sulfur restriction is leading to decreases in the maximum sulfur content of fuel used, but are having minimal influence on the average (Mestl et al., 2013).

ACPD
13, 24635–24674, 2013

3.1.5 Influence of vessel speed on emission

Opportunities to measure emissions from individual in-operation vessels, especially as a function of vessel speed, are rare and, as such, only a handful of case-studies are available (Agrawal et al., 2008a,b, 2010; Jayaram et al., 2011; Khan et al., 2012a,b; Lack et al., 2011). This is particularly true for measurements of compositionally-resolved PM emissions and for inter-comparisons of different techniques measuring the same pollutant.

Although decreased absolute emissions are expected as a result of the fuel economy increase as a vessel slows, there is not yet a clear understanding of how changes to vessel speed influences fuel-based emissions factors (EFs), i.e. the amount of pollutant emitted per kg fuel burned, although various studies using either laboratory test-rigs or in use stack sampling have provided insights (Agrawal et al., 2008a,b, 2010; Jayaram et al., 2011; Khan et al., 2012a, b; Petzold et al., 2008, 2010, 2011a). If EFs vary with vessel speed, then they may either enhance or decrease the effect of the increased fuel economy on the actual emissions (E_X) because:

$$E_X = \frac{EF_X}{F_{econ}} \times D \quad (2)$$

where EF_X is the emission factor for pollutant X (in amount of X per kg fuel), D is the total distance travelled and E_X is the absolute emissions; both EF_X and F_{econ} may be vessel speed dependent.

For the *Miller Freeman* the EF_{POM} and EF_{BC} both increase with vessel speed (Fig. 1). Since the emitted PM_1 is dominated by POM and BC, EF_{PM_1} also increases with vessel speed. There have been a few previous measurements of vessel speed effects (or more commonly, engine load effects) on EF_{BC} for individual ships as measured in-stack (Agrawal et al., 2008a,b, 2010; Jayaram et al., 2011; Khan et al., 2008, 2012a,b), for individual test rigs (Petzold et al., 2008, 2010, 2011a; Kasper et al., 2007; Sarvi and Zevenhoven, 2010; Sarvi et al., 2009) or for an ensemble of different ships using the

ACPD
13, 24635–24674, 2013

plume intercept method (Lack et al., 2008b). (Note that some of these studies actually report EF_{EC}, where EC is elemental carbon. EC is similar to, but not identical to BC, as both are defined based on the measurement method used. We assume here that EF_{BC} is interchangeable with EF_{EC}. See Petzold et al. (2013) for an extensive discussion.) These studies encompass slow, medium and high-speed diesel engines (SSD, MSD and HSD, respectively) of various types and a variety of different fuel types, including HFO, MGO, MDO and various biofuels. Most of the studies were done on vessels/engines substantially newer than the *Miller Freeman*. Propeller type was not reported for any of the in-stack studies, although for the in-stack studies that investigated larger ocean going vessels it is likely that they operated fixed pitch propellers. (Propeller type does not apply to test-rig studies.) These differences present some challenges in making comparisons between different studies, including between the current study and the literature results. Nonetheless, it is instructional to consider the dependence observed here in the context of the literature results to gain insights into how differences in operation influence emissions, and absolute values can be compared independent of the actual speed dependence. We assume that for the literature studies the propeller law provides a reasonable method by which the ship speed (or potential ship speed, in the case of test-rig studies) can be estimated, or more specifically the ratio between the operating speed and the maximum speed (referred to here as the speed ratio). Therefore, the engine load values reported for the literature in-stack and test-rig studies have been converted to speed ratio values using the propeller law.

Adopting the approach of Lack and Corbett (2012) we present literature EF_{BC} (and EF_{EC}) vs. speed ratio (either directly measured or estimated from the propeller law), and where either the absolute values of EF_{BC} are considered (Fig. 5b) or where the EF_{BC} values have been normalized to 95 % of their maximum speed (equivalent to 85 % load from the propeller law; Fig. 5a). It is important to compare EFs in the same units (here g kg-fuel^{-1}), and thus the literature results have been converted to g kg-fuel^{-1} from g kW^{-1} h^{-1}, as necessary (see Supplement for details of this conversion). It is evident that there is a great deal of scatter in the combined observations regarding the de-

ACPD
13, 24635–24674, 2013

pendence of EF_{BC} on speed and it is difficult to develop generalized results, although it is clear that the *Miller Freeman* exhibits substantially different behavior than most other engines/vessels considered. This may be due to differences in propeller type between the *Miller Freeman* and other vessels. The absolute EF_{BC} values at higher speed ratios for the *Miller Freeman* are somewhat larger than most of the other individual ship studies, although are within the multi-ship range of values observed by Lack et al. (2009) and are comparable to observations for other vessels encountered during CalNex (Buffaloe et al., 2013). At lower speed ratios the *Miller Freeman* EF_{BC} are well within the range of the individual ship studies.

Considering the literature results all together, there appears to be no clear distinction between studies that utilize SSD vs. MSD engines, or between those that use HFO vs. LSF. There does appear to be some small distinction between the majority of test rig studies and the majority of stack sampling studies; most test rig studies (with the exception of Kasper et al., 2007) indicate a decrease in EF_{BC} with increasing speed ratio while most stack sampling studies (with the exception of Jayaram et al., 2011) suggest flat or slightly decreasing EF_{BC} with speed ratio.

The present work is the only plume-intercept study that involved a single ship and is most consistent with the Kasper et al. (2007) lab study and the Jayaram et al. (2011) stack sampling study (with the exception of the lowest speed ratio, which for Jayaram et al. was for "idle" while in ours was slow travel). The reason for the apparent similarity of the current work with these particular studies is not clear because they had used the same, or very similar, sampling methodologies as the other stack sampling and test rig studies. This may simply be an indication of the study-to-study variability. The ensemble study of Lack et al. (2008b), in which EFs were determined from plume intercepts from multiple ships (excluding tugs), with each ship typically sampled at one single speed, does not suggest a clear dependence of EF_{BC} on speed; this may simply reflect that the ship-to-ship variability is larger than any vessel speed/engine load effect and demonstrates the need for further studies that focus on the behavior of individual vessels.

ACPD
13, 24635–24674, 2013

Literature results for EF_{POM} (or EF_{POC}, where POC is particulate organic carbon, i.e. POM excluding the mass of non-C atoms) as a function of speed ratio are shown normalized to 85 % (Fig. 6a) or as absolute values (Fig. 6b). As with EF_{BC}, there is a great deal of scatter in the EF_{POM}/speed relationships, although with most literature studies suggesting an increase or being relatively flat in the EF_{POM} at low speed ratios, different than the current study. This may reflect differences in engine/vessel operating conditions. Our results are again most consistent with the test-rig MGO results from Kasper et al. (2007), who observed an increase in EF_{POM} with estimated speed. Also as with EF_{BC}, there is a great deal of scatter between the various studies in terms of the absolute EF_{POM} values. As discussed in Sect. 3.1.2, EF_{POM} measurements may be influenced by the extent of dilution during sampling, although it is not clear how this might influence observations of the EF_{POM}/speed dependence.

Despite the large number of points in Figs. 5 and 6, only a handful of different engines have actually been tested, which leaves an open question of the general dependence of EF_{BC} and EF_{POM} on vessel speed (and engine load), or whether generalizations can even be determined. We suggest more plume intercept studies targeting individual vessels would be beneficial, although coordinating such studies for measurement of emissions from individual vessels (as in this study) is extremely difficult, requiring multiple platforms. Additionally, use of a variety of instrumentation to measure BC (or EC) is suggested.

3.2 Gas phase emissions

EFs for gas-phase species are shown in Fig. 7 and given in Table 1. EF_{CO} decreased with increasing vessel speed by approximately a factor of 3 over the range considered here. In contrast, EF_{NO_x} increased with increasing vessel speed by approximately 20 %. These results are expected since higher speed operation would likely have resulted in higher peak combustion temperatures and, therefore, greater NO formation and lower CO production. Since diesel engines typically operate under fuel lean conditions, if the fuel-to-air ratio did increase with vessel speed, as we postulated earlier,

ACPD
13, 24635–24674, 2013

this would likely accentuate the NO_x increase but have minimal influence on CO. The EF_{HCHO} are inversely correlated with F_{load}. For all but the lowest speed plume, the relationship between EF_{CO} and EF_{HCHO} is consistent with previous observations from Williams et al. (2009). Our observations of EF_{NO_x} and EF_{CO} exhibit the opposite dependence of that observed by Khan et al. (2012a) for operation of a SSD engine on MGO, although agree with their observations when the ship operated on HFO. For comparison, Agrawal et al. (2010) found little dependence of CO or NO_x EFs on engine load for a SSD container ship operating on HFO. The reason for these differences is unclear, but could be related to engine or propeller type. Our results for CO suggest that, for smaller vessels such as the *Miller Freeman*, the decrease in absolute emissions from increased fuel economy at reduced speeds may be offset to some extent by an increase in EF_{CO}, whereas the decrease in EF_{NO_x} may enhance emissions reductions.

The values of EF_{SO_2} were independent of vessel speed. We would not expect EF_{SO_2} to depend strongly on engine load since it is primarily dependent on the sulfur content of the fuel. This is similar behavior as observed by Khan et al. (2012a). The low value of EF_{SO_2} confirms that *Miller Freeman* was indeed burning low sulfur fuel, which we estimate to be 0.097 ± 0.011 % S by weight based upon the average EF_{SO_2}, a negligible EF for p-SO_4^{2-} and the assumption that SO_3 emissions are very small.

4 Implications

Our results provide a useful case study of the dependence of PM and trace gas emissions factors on vessel speed as measured from a real-world MSD vessel, representative of many harbor craft vessels operating on low-sulfur fuel. The observed increase in PM mass EFs with vessel speed suggests that slower speed operation of these vessel types may lead to substantially lower emissions, especially since slower speed operation also corresponds to (typically) better fuel economy. One aspect not considered here is that harbor craft vessels operating near-shore or in inland waterways may be subject to frequent speed changes, and we do not have measurements as to how the

ACPD
13, 24635–24674, 2013

EFs respond to rapid acceleration; we suggest such measurements would be useful in future studies.

More broadly, comparison with literature results demonstrates that challenges exist in developing a generalized EF/speed (or engine load) relationship, in particular for PM emissions, because results from individual studies may depend on the measurement methodology used: plume intercept (this study and others, Lack et al., 2008b, 2009, 2011; Petzold et al., 2008) versus in-use stack sampling (Agrawal et al., 2008a, 2010; Jayaram et al., 2011; Khan et al., 2012a,b; Murphy et al., 2009) versus test rig sampling (Petzold et al., 2010, 2011a; Sarvi et al., 2009; Sarvi and Zevenhoven, 2010; Kasper et al., 2007). This is true even if the current study is excluded. Also, it is clear that there is a great deal of variability in the absolute emissions between different vessels, perhaps not surprising given the variety of different engine types and ages considered in the various studies (Table S1). Methodological limitations, along with the limited number of different vessels or engines for which measurements have been made, makes it difficult to establish whether engine type or fuel type affects the EF/speed relationship. Although logistically more challenging, we suggest that plume intercept studies, which allow for measurement of EFs under actual atmospheric dilution conditions, may provide for EFs that are most relevant to the actual atmosphere, and thus to emission inventory development. We additionally suggest that, whenever possible, multiple measurement techniques be employed, especially for BC (or EC). Our measurement of BC EFs at atmospheric relevant dilution levels using multiple methodologies (e.g. photo-acoustics, filter-based absorption, laser induced incandescence and aerosol mass spectrometry) suggest that the SP2 underestimates BC emissions relative to other methods, likely due to methodological limitations. We suggest that, barring additional improvements in field-deployable laser induced incandescence methods (e.g. Chan et al., 2011), that light absorption techniques may provide the most robust and accurate determination of EF_{BC}. Further consideration of the influence of vessel speed and engine load on other engine and ship types remains necessary.

ACPD
13, 24635–24674, 2013

Supplementary material related to this article is available online at http://www.atmos-chem-phys-discuss.net/13/24635/2013/acpd-13-24635-2013-supplement.pdf.

Acknowledgements. The authors thank the crews of the R/V *Atlantis* and the *Miller Freeman,* especially the Field Operations Officer on the *Miller Freeman* LT Patrick Murphy, without all of whom this study would not have been possible. This work was supported in part by the US Environmental Protection Agency under a STAR research assistance agreement (RD834558), the NOAA Climate Program (including NA09OAR4310124 and NA09AR4310125), the California Air Resources Board, the Canadian Federal Government (PERD Project C12.007) and NSERC. It has not been formally reviewed by the any of the funding agencies. The views expressed in this document are solely those of the authors, and the funding agencies do not endorse any products or commercial services mentioned in this publication.

References

Agrawal, H., Malloy, Q. G. J., Welch, W. A., Wayne Miller, J., and Cocker III, D. R.: In-use gaseous and particulate matter emissions from a modern ocean going container vessel, Atmos. Environ., 42, 5504–5510, doi:10.1016/j.atmosenv.2008.02.053, 2008a.

Agrawal, H., Welch, W. A., Miller, J. W., and Cocker III, D. R.: Emission measurements from a crude oil tanker at sea, Environ. Sci. Technol., 42, 7098–7103, doi:10.1021/es703102y, 2008b.

Agrawal, H., Welch, W. A., Henningsen, S., Miller, J. W., and Cocker III, D. R.: Emissions from main propulsion engine on container ship at sea, J. Geophys. Res.-Atmos., 115, D23205, doi:10.1029/2009jd013346, 2010.

Arneth, A., Unger, N., Kulmala, M., and Andreae, M. O.: Clean the Air, Heat the Planet?, Science, 326, 672–673, doi:10.1126/science.1181568, 2009.

Bond, T. C. and Bergstrom, R. W.: Light absorption by carbonaceous particles: An investigative review, Aerosol Sci. Tech., 40, 27–67, doi:10.1080/02786820500421521, 2006.

ACPD
13, 24635–24674, 2013

Buffaloe, G., Onasch, T. B., Massoli, P., Li, S. M., Hayden, K., Nuaanman, I., Williams, E., Lack, D. A., and Cappa, C. D.: Black carbon emissions from in use ships: Results from CalNex 2010, in preparation, 2013.
Buhaug, O., Corbett, J. J., Endresen, O., Eyring, V., Faber, J., Hanayama, S., Lee, D. S., Lee, D., Lindstad, H., Mjelde, A., Palsson, C., Wanquing, W., Winebrake, J. J., and Yoshida, K.: Second IMO Greenhouse Gas Study, International Maritime Organization, London, 2009.
California Air Resources Board, Final Regulation Order. Fuel Sulfur and Other Operational Requirements for Ocean-Going Vessels Within California Waters and 24 Nautical Miles of the California Baseline: http://www.arb.ca.gov/regact/2011/ogv11/ogvfro13.pdf, last access: 17 June 2013, 2011.
Canagaratna, M. R., Jayne, J. T., Jimenez, J. L., Allan, J. D., Alfarra, M. R., Zhang, Q., Onasch, T. B., Drewnick, F., Coe, H., Middlebrook, A., Delia, A., Williams, L. R., Trimborn, A. M., Northway, M. J., DeCarlo, P. F., Kolb, C. E., Davidovits, P., and Worsnop, D. R.: Chemical and microphysical characterization of ambient aerosols with the aerodyne aerosol mass spectrometer, Mass Spectrom. Rev., 26, 185–222, doi:10.1002/mas.20115, 2007.
Cappa, C. D., Lack, D. A., Burkholder, J. B., and Ravishankara, A. R.: Bias in filter-based aerosol light absorption measurements due to organic aerosol loading: Evidence from laboratory measurements, Aerosol Sci. Tech., 42, 1022–1032, doi:10.1080/02786820802389285, 2008.
Chan, T. W., Brook, J. R., Smallwood, G. J., and Lu, G.: Time-resolved measurements of black carbon light absorption enhancement in urban and near-urban locations of southern Ontario, Canada, Atmos. Chem. Phys., 11, 10407–10432, doi:10.5194/acp-11-10407-2011, 2011.
Corbett, J. J. and Fischbeck, P. S.: Emissions from Waterborne Commerce Vessels in United States Continental and Inland Waterways, Environ. Sci. Technol., 34, 3254–3260, doi:10.1021/es9911768, 2000.
Corbett, J. J., Winebrake, J. J., Green, E. H., Kasibhatla, P., Eyring, V., and Lauer, A.: Mortality from Ship Emissions: A Global Assessment, Environ. Sci. Technol., 41, 8512–8518, doi:10.1021/es071686z, 2007.
Corbett, J. J., Wang, H., and Winebrake, J. J.: The effectiveness and costs of speed reductions on emissions from international shipping, Transport Res. D-Tr. E, 14, 593–598, doi:10.1016/j.trd.2009.08.005, 2009.
DeCarlo, P. F., Slowik, J. G., Worsnop, D., Davidovits, P., and Jimenez, J. L.: Particle morphology and density characterization by combined mobility and aerodynamic diameter measure-

ACPD
13, 24635–24674, 2013

ments. Part 1: Theory, Aerosol Sci. Tech., 38, 1185–1205, doi:10.1080/027868290903907, 2004.
Equasis, The World Merchant Fleet in 2011, Statistics from Equasis: www.emsa.europa.eu/news-a-press-centre/download/1933/1554/23.html, last access: 21 May 2013, 2012.
Fuglestvedt, J., Berntsen, T., Eyring, V., Isaksen, I., Lee, D. S., and Sausen, R.: Shipping Emissions: From Cooling to Warming of Climate – and Reducing Impacts on Health, Environ. Sci. Technol., 43, 9057–9062, doi:10.1021/es901944r, 2009.
Fujitani, Y., Saitoh, K., Fushimi, A., Takahashi, K., Hasegawa, S., Tanabe, K., Kobayashi, S., Furuyama, A., Hirano, S., and Takami, A.: Effect of isothermal dilution on emission factors of organic carbon and n-alkanes in the particle and gas phases of diesel exhaust, Atmos. Environ., 59, 389–397, doi:10.1016/j.atmosenv.2012.06.010, 2012.
Hand, J. L. and Malm, W. C.: Review of aerosol mass scattering efficiencies from ground-based measurements since 1990, J. Geophys. Res.-Atmos., 112, D16203, doi:10.1029/2007JD008484, 2007.
Huffman, J. A., Jayne, J., Drewnick, F., Aiken, A. C., Onasch, T., and Worsnop, D.: Design, modeling, optimization and experimental tests of a particle beam width probe for the Aerodyne aerosol mass spectrometer, Aerosol Sci. Technol., 39, 1143–1163, doi:10.1080/02786820500423782, 2005.
Jayaram, V., Agrawal, H., Welch, W. A., Miller, J. W., and Cocker, D. R.: Real-Time Gaseous, PM and Ultrafine Particle Emissions from a Modern Marine Engine Operating on Biodiesel, Environ. Sci. Technol., 45, 2286–2292, doi:10.1021/es1026954, 2011.
Kasper, A., Aufdenblatten, S., Forss, A., Mohr, M., and Burtscher, H.: Particulate Emissions from a Low-Speed Marine Diesel Engine, Aerosol Sci. Tech., 41, 24–32, doi:10.1080/02786820601055392, 2007.
Khan, M. Y., Giordano, M., Gutierrez, J., Welch, W. A., Asa-Awuku, A., Miller, J. W., and Cocker, D. R.: Benefits of two mitigation strategies for container vessels: cleaner engines and cleaner fuels, Environ. Sci. Technol., 46, 5049–5056, doi:10.1021/es2043646, 2012a.
Khan, M. Y., Russell, R. L., Welch, W. A., Cocker, D. R., and Ghosh, S.: Impact of Algae Biofuel on In-Use Gaseous and Particulate Emissions from a Marine Vessel, Energy & Fuels, 26, 6137–6143, doi:10.1021/ef300935z, 2012b.
Laborde, M., Mertes, P., Zieger, P., Dommen, J., Baltensperger, U., and Gysel, M.: Sensitivity of the Single Particle Soot Photometer to different black carbon types, Atmos. Meas. Tech., 5, 1031–1043, doi:10.5194/amt-5-1031-2012, 2012.

ACPD
13, 24635–24674, 2013

Lack, D. A. and Corbett, J. J.: Black carbon from ships: a review of the effects of ship speed, fuel quality and exhaust gas scrubbing, Atmos. Chem. Phys., 12, 3985–4000, doi:10.5194/acp-12-3985-2012, 2012.

Lack, D. A., Cappa, C. D., Covert, D. S., Baynard, T., Massoli, P., Sierau, B., Bates, T. S., Quinn, P. K., Lovejoy, E. R., and Ravishankara, A. R.: Bias in filter-based aerosol light absorption measurements due to organic aerosol loading: Evidence from ambient measurements, Aerosol Sci. Tech., 42, 1033–1041, doi:10.1080/02786820802389277, 2008a.

Lack, D. A., Lerner, B., Granier, C., Baynard, T., Lovejoy, E., Massoli, P., Ravishankara, A. R., and Williams, E.: Light absorbing carbon emissions from commercial shipping, Geophys. Res. Lett., 35, L13815, doi:10.1029/2008gl033906, 2008b.

Lack, D. A., Corbett, J. J., Onasch, T., Lerner, B., Massoli, P., Quinn, P. K., Bates, T. S., Covert, D. S., Coffman, D., Sierau, B., Herndon, S., Allan, J., Baynard, T., Lovejoy, E., Ravishankara, A. R., and Williams, E.: Particulate emissions from commercial shipping: Chemical, physical, and optical properties, J. Geophys. Res.-Atmos., 114, D00F04, doi:10.1029/2008jd011300, 2009.

Lack, D. A., Cappa, C. D., Langridge, J., Bahreni, R., Buffaloe, G., Brock, C. A., Cerully, K., Hayden, K., Holloway, J. S., Lerner, B., Li, S. M., McLaren, R., Middlebrook, A., Moore, R., Nenes, A., Nuaanman, I., Peischl, J., Perring, A., Quinn, P. K., Ryerson, T. B., Schwarz, J. P., Spackman, J. R., and Williams, E. J.: Impact of Fuel Quality Regulation and Speed Reductions on Shipping Emissions: Implications for Climate and Air Quality, Environ. Sci. Technol., 45, 9052–9060, doi:10.1021/es2013424, 2011.

Lack, D. A., Richardson, M. S., Law, D., Langridge, J. M., Cappa, C. D., and Murphy, D. M.: Aircraft instrumentation for comprehensive characterization of aerosol optical properties, Part 2: Black and brown carbon absorption and absorption enhancement measured with photo acoustic spectroscopy, Aerosol Sci. Tech., 46, 555–568, doi:10.1080/02786820600803917, 2012.

Langridge, J. M., Richardson, M. S., Lack, D., Law, D., and Murphy, D. M.: Aircraft Instrument for Comprehensive Characterization of Aerosol Optical Properties, Part I: Wavelength-Dependent Optical Extinction and Its Relative Humidity Dependence Measured Using Cavity Ringdown Spectroscopy, Aerosol Sci. Tech., 45, 1305–1318, doi:10.1080/02786826.2011.592745, 2011.

Lauer, A., Eyring, V., Corbett, J. J., Wang, C., and Winebrake, J. J.: Assessment of Near-Future Policy Instruments for Oceangoing Shipping: Impact on Atmospheric Aerosol

ACPD
13, 24635–24674, 2013

Burdens and the Earth's Radiation Budget, Environ. Sci. Technol., 43, 5592–5598, doi:10.1021/es900922h, 2009.
Liggio, J., Gordon, M., Smallwood, G., Li, S.-M., Stroud, C., Staebler, R., Lu, G., Lee, P., Taylor, B., and Brook, J. R.: Are Emissions of Black Carbon from Gasoline Vehicles Underestimated? Insights from Near and On-Road Measurements, Environ. Sci. Technol., 46, 4819–4828, doi:10.1021/es2033845, 2012.
Lipsky, E. M. and Robinson, A. L.: Effects of dilution on fine particle mass and partitioning of semivolatile organics in diesel exhaust and wood smoke, Environ. Sci. Technol., 40, 155–162, doi:10.1021/es050319p, 2006.
Lloyd's Register Engineering Services: Marine Exhaust Emissions Research Programme, London, 1995.
Matthew, B. M., Middlebrook, A. M., and Onasch, T. B.: Collection efficiencies in an Aerodyne Aerosol Mass Spectrometer as a function of particle phase for laboratory generated aerosols, Aerosol Sci. Tech., 42, 884–898, doi:10.1080/02786820802356797, 2008.
McLaren, R., Wojtal, P., Halla, J. D., Mihele, C., and Brook, J. R.: A survey of NO_2:SO_2 emission ratios measured in marine vessel plumes in the Strait of Georgia, Atmos. Environ., 46, 655–658, doi:10.1016/j.atmosenv.2011.10.044, 2012.
Mestl, T., Løvoll, G., Stensrud, E., and Le Breton, A.: The Doubtful Environmental Benefit of Reduced Maximum Sulfur Limit in International Shipping Fuel, Environ. Sci. Technol., doi:10.1021/es4009954, 2013.
Murphy, S. M., Agrawal, H., Sorooshian, A., Padroi, L. T., Gates, H., Hersey, S., Welch, W. A., Jung, H., Miller, J. W., Cocker, D. R., Nenes, A., Jonsson, H. H., Flagan, R. C., and Seinfeld, J. H.: Comprehensive Simultaneous Shipboard and Airborne Characterization of Exhaust from a Modern Container Ship at Sea, Environ. Sci. Technol., 43, 4626–4640, doi:10.1021/es802413j, 2009.
NOAA, Miller Freeman: http://www.moc.noaa.gov/mf/apr_2004_mf_specs.pdf, last access: 10 January 2011, 2010.
Onasch, T. B., Trimborn, A. M., Fortner, E. C., Jayne, J. T., Kok, G. L., WilliamS, L. R., Davidovits, P., and Worsnop, D. R.: Soot Particle Aerosol Mass Spectrometer: Development, Validation and Initial Application, Aerosol Sci. Tech., 46, 804–817, doi:10.1080/02786826.2012.663948, 2012.
Petzold, A., Hasselbach, J., Lauer, P., Baumann, R., Franke, K., Gurk, C., Schlager, H., and Weingartner, E.: Experimental studies on particle emissions from cruising ship, their char-

ACPD
13, 24635–24674, 2013

acteristic properties, transformation and atmospheric lifetime in the marine boundary layer, Atmos. Chem. Phys., 8, 2387–2403, doi:10.5194/acp-8-2387-2008, 2008.
Petzold, A., Weingartner, E., Hasselbach, I., Lauer, P., Kurok, C., and Fleischer, F.: Physical Properties, Chemical Composition, and Cloud Forming Potential of Particulate Emissions from a Marine Diesel Engine at Various Load Conditions, Environ. Sci. Technol., 44, 3800–3805, doi:10.1021/es903681z, 2010.
Petzold, A., Lauer, P., Fritsche, U., Hasselbach, J., Lichtenstern, M., Schlager, H., and Fleischer, F.: Operation of Marine Diesel Engines on Biogenic Fuels: Modification of Emissions and Resulting Climate Effects, Environ. Sci. Technol., 45, 10394–10400, doi:10.1021/es2021439, 2011a.
Petzold, A., Marsh, R., Johnson, M., Miller, M., Sevcenco, Y., Delhaye, D., Ibrahim, A., Williams, P., Bauer, H., Crayford, A., Bachalo, W. D., and Raper, D.: Evaluation of Methods for Measuring Particulate Matter Emissions from Gas Turbines, Environ. Sci. Technol., 45, 3562–3568, doi:10.1021/es103969v, 2011b.
Petzold, A., Ogren, J. A., Fiebig, M., Laj, P., Li, S. M., Baltensperger, U., Holzer-Popp, T., Kinne, S., Pappalardo, G., Sugimoto, N., Wehrli, C., Wiedensohler, A., and Zhang, X. Y.: Recommendations for the interpretation of "black carbon" measurements, Atmos. Chem. Phys. Discuss., 13, 9485–9517, doi:10.5194/acpd-13-9485-2013, 2013.
Pierce, J. R., and Adams, P. J.: Efficiency of cloud condensation nuclei formation from ultrafine particles, Atmos. Chem. Phys., 7, 1367–1379, doi:10.5194/acp-7-1367-2007, 2007.
Roberts, G. C., and Nenes, A.: A continuous-flow streamwise thermal-gradient CCN chamber for atmospheric measurements, Aerosol Sci. Tech., 39, 206–221, doi:10.1080/027868290913988, 2005.
Ryerson, T. B., Andrews, A. E., Angevine, W. M., Bates, T. S., Brock, C. A., Cairns, B., Cohen, R. C., Cooper, O. R., De Gouw, J. A., Fehsenfeld, F. C., Ferrare, R. A., Fischer, M. L., Flagan, R. C., Goldstein, A. H., Hair, J. W., Hardesty, R. M., Hostetler, C. A., Jimenez, J. L., Langford, A. O., McCauly, E., McKeen, S. A., Molina, L. T., Nenes, A., Oltmans, S. J., Parrish, D. D., Pederson, J. R., Pierce, R. B., Prather, K., Quinn, P. K., Seinfeld, J. H., Senff, C. J., Sorooshian, A., Stutz, J., Surratt, J. D., Trainer, M., Volkamer, R. M., WIlliams, E. J., and Wofsy, S. C.: The 2010 California Research at the Nexus of AIr Quality and Climate Change (CalNex) Field Study, J. Geophys. Res.-Atmos., accepted, doi:10.1002/jgrd.50331, 2013.
Sarvi, A. and Zevenhoven, R.: Large-scale diesel engine emission control parameters, Energy, 35, 1139–1145, doi:10.1016/j.energy.2009.06.007, 2010.

ACPD
13, 24635–24674, 2013

Sarvi, A., Kilpinen, P., and Zevenhoven, R.: Emissions from large-scale medium-speed diesel engines: 3. Influence of direct water injection and common rail, Fuel Process. Technol., 90, 222–231, doi:10.1016/j.fuproc.2008.09.003, 2009.

Schwarz, J. P., Gao, R. S., Fahey, D. W., Thomson, D. S., Watts, L. A., Wilson, J. C., Reeves, J. M., Darbeheshti, M., Baumgardner, D. G., Kok, G. L., Chung, S. H., Schulz, M., Hendricks, J., Lauer, A., Karcher, B., Slowik, J. G., Rosenlof, K. H., Thompson, T. L., Langford, A. O., Loewenstein, M., and Aikin, K. C.: Single-particle measurements of midlatitude black carbon and light-scattering aerosols from the boundary layer to the lower stratosphere, J. Geophys. Res.-Atmos., 111, D16207, doi:10.1029/2006jd007076, 2006.

Schwarz, J. P., Spackman, J. R., Gao, R. S., Perring, A. E., Cross, E., Onasch, T. B., Ahern, A., Wrobel, W., Davidovits, P., Olfert, J., Dubey, M. K., Mazzoleni, C., and Fahey, D. W.: The Detection Efficiency of the Single Particle Soot Photometer, Aerosol Sci. Tech., 44, 612–628, doi:10.1080/02786826.2010.481298, 2010.

U.S. EPA, Designation of North American Emission Control Area to Reduce Emissions from Ships, EPA-420-F-10-015: http://www.epa.gov/otaq/regs/nonroad/marine/ci/420f10015.pdf, last access: 23 March 2013, 2010.

United Nations Conference on Trade and Development: Structure, Ownership and Registration of the World Fleet, in: Review of Maritime Transport, 2011.

Virkkula, A., Ahlquist, N. C., Covert, D. S., Arnott, W. P., Sheridan, P. J., Quinn, P. K., and Coffman, D. J.: Modification, calibration and a field test of an instrument for measuring light absorption by particles, Aerosol Sci. Tech., 39, 68–83, doi:10.1080/027868290901963, 2005.

Wang, H. and Minjares, R.: Global emissions of marine black carbon: critical review and revised assessment, 92nd Transportation Research Board Annual Meeting, http://docs.trb.org/prp/13-1503.pdf, 2013.

Williams, E. J., Lerner, B. M., Murphy, P. C., Herndon, S. C., and Zahniser, M. S.: Emissions of NO_x, SO_2, CO, and HCHO from commercial marine shipping during Texas Air Quality Study (TexAQS) 2006, J. Geophys. Res.-Atmos., 114, D21306, doi:10.1029/2009jd012094, 2009.

ACPD
13, 24635–24674, 2013

Table 1. Measured emissions factors for the NOAA Ship *Miller Freeman* as a function of vessel speed.

Speed	2.9 knots	6.9 knots	6.9 knots	10.2 knots	12 knots	units
Approx. Plume age	5	2	1	1	3	min
			Gas Phase			
NO_x[1]	45.6 ± 8.2	45.7 ± 8.2		53.3 ± 9.6	61.1 ± 11.0	g kg-fuel^{-1}
SO_2	1.85 ± 0.5	1.76 ± 0.44		1.88 ± 0.47	2.27 ± 0.57	g kg-fuel^{-1}
CO	6.23 ± 1.2	5.83 ± 0.9		2.92 ± 0.58	2.50 ± 0.50	g kg-fuel^{-1}
HCHO	0.25± 0.04	0.125 ± 0.02		0.058 ± 0.01	0.056 ± 0.02	g kg-fuel^{-1}
			Particle phase			
SO_4^{2-} (HR-AMS)	< 0.05	< 0.15	< 0.09	< 0.10	< 0.13	g kg-fuel^{-1}
SO_4^{2-} (SP-AMS)	< 0.03	< 0.06	< 0.05	< 0.05	< 0.07	g kg-fuel^{-1}
OM (HR-AMS)	0.07	0.10	0.18	0.47	1.13	g kg-fuel^{-1}
OM (SP-AMS)	< 0.03	0.19	0.23	0.53	0.86	g kg-fuel^{-1}
OM (Wt. Ave)	0.05	0.10	0.18	0.47	1.10	g kg-fuel^{-1}
NO_3^- (HR-AMS)	< 0.004	< 0.012	< 0.008	< 0.006	< 0.011	g kg-fuel^{-1}
NO_3^- (SP-AMS)	< 0.002	< 0.004	< 0.004	< 0.003	< 0.005	g kg-fuel^{-1}
NH_4^+ (HR-AMS)	< 0.02	< 0.07	< 0.03	< 0.04	< 0.05	g kg-fuel^{-1}
NH_4^+ (SP-AMS)	< 0.004	< 0.006	0.003	0.003	< 0.009	g kg-fuel^{-1}
Cl^- (HR-AMS)	< 0.002	< 0.005	< 0.003	< 0.004	0.002	g kg-fuel^{-1}
Cl^- (SP-AMS)	< 0.002	< 0.004	< 0.003	< 0.003	0.003	g kg-fuel^{-1}
BC (SP2)	0.008	0.09	0.11	0.30	0.16	g kg-fuel^{-1}
BC (SP-AMS)	0.06	0.15	0.14	0.34	0.43	g kg-fuel^{-1}
BC (PAS,G)[2]	0.04	0.14	0.20	0.39	0.41	g kg-fuel^{-1}
BC (PAS,B)[3]	0.16	0.19	0.27	0.47	0.52	g kg-fuel^{-1}
BC (PSAP, Ave)[4]	0.04	0.19	0.23	0.49	0.48	g kg-fuel^{-1}
BC (Wt. Ave)	0.04	0.15	0.20	0.41	0.41	g kg-fuel^{-1}
CN (> 12 nm)	1.33×10^{16}	1.04×10^{16}	1.61×10^{16}	1.95×10^{16}	1.48×10^{16}	# kg-fuel^{-1}
CN (> 3 nm)	1.93×10^{16}	1.72×10^{16}	2.65×10^{16}	3.06×10^{16}	2.23×10^{16}	# kg-fuel^{-1}
CCN[5] (SS = 0.7 %)	2.6×10^{14}	–	3.6×10^{14}	–	1.7×10^{14}	# kg-fuel^{-1}
CCN (SS = 0.6 %)	8.3×10^{13}	–	7.0×10^{13}	–	6.3×10^{13}	# kg-fuel^{-1}
CCN (SS = 0.4 %)	–	2.7×10^{13}	–	–	–	# kg-fuel^{-1}
CCN (SS = 0.3 %)	–	–		$< 1 \times 10^{13}$	–	# kg-fuel^{-1}
CCN/CN[6] (SS = 0.7 %)	0.021	–	0.019	–	0.008	unitless
CCN/CN (SS = 0.6 %)	0.007	–	0.004	–	0.004	unitless
CCN/CN (SS = 0.4 %)	–	0.002	–	–	–	unitless
CCN/CN (SS = 0.3 %)	–	–	–	$< 4 \times 10^{-4}$	–	unitless
Extinction	0.83	1.60	2.10	3.37	4.05	Mm^{-1} kg^{-1} fuel
PM_1 (ext.)[7]	0.21	0.40	0.52	0.84	1.01	g kg-fuel^{-1}
PM_1 (sum)[8]	0.09	0.25	0.38	0.88	1.51	g kg-fuel^{-1}
$D_{p,m}^9$	30	–	–	48	69	nm

[1] Calculated as equivalent NO_2; [2] Assumes MAE = 7.75 m^2 g^{-1}; [3] Assumes MAE = 10.2 m^2 g^{-1}; [4] Assumes MAE = 7.5 m^2 g^{-1}; [5] CCN measurements may only be for a portion of a given plume due to the time-dependent supersaturation; [6] CCN/CN ratios have been calculated after determining CN EFs over the same period as the CCN, and therefore may not correspond to the reported plume-average CN EFs; [7] Assumes MEE = 4 m^2 g^{-1}; [8] $[PM_1] = [OM]_{ave} + [BC]_{ave}$; [9] Number weighted mobility diameter; [10] Values reported as < X are the plume-specific detection limit.

ACPD
13, 24635–24674, 2013

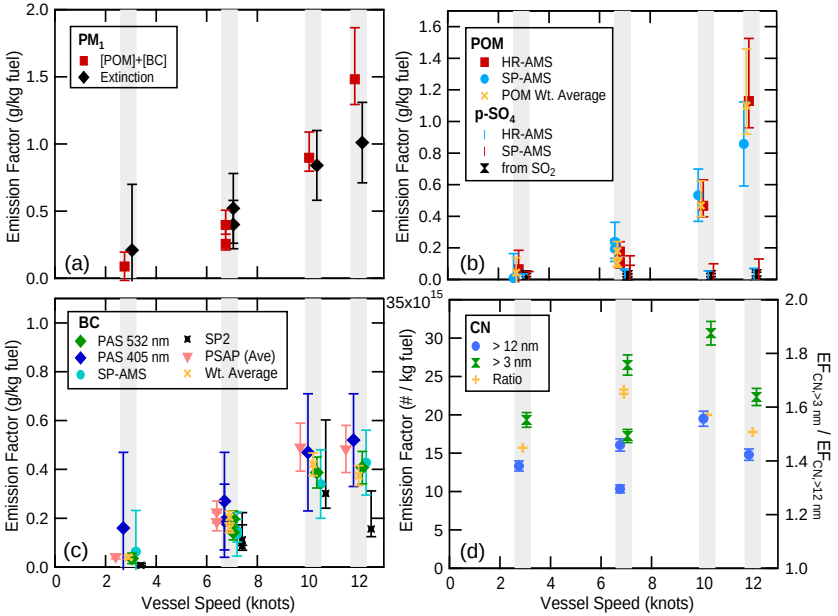

Fig. 1. Measured mass or number-based emissions factors (in per kg-fuel) for **(a)** total sub-micron particulate matter, **(b)** POM or particulate SO_4, **(c)** BC and **(d)** condensation nuclei. Values have been offset from the central speed, indicated in gray, for clarity. For sulfate, error bars shown with no data point indicate the plume-specific detection limit for that species.

ACPD
13, 24635–24674, 2013

A case study into the measurement of ship emissions

C. D. Cappa et al.

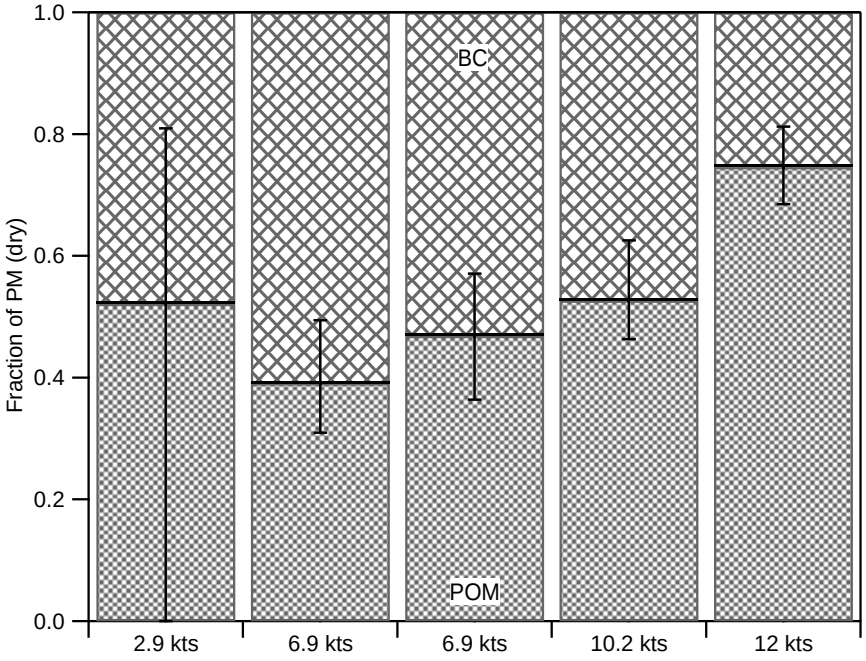

Fig. 2. The fraction of PM_1 that is BC (cross-hatched) or POM (solid) as a function of vessel speed, determined from the weighted average POM and BC EFs.

ACPD
13, 24635–24674, 2013

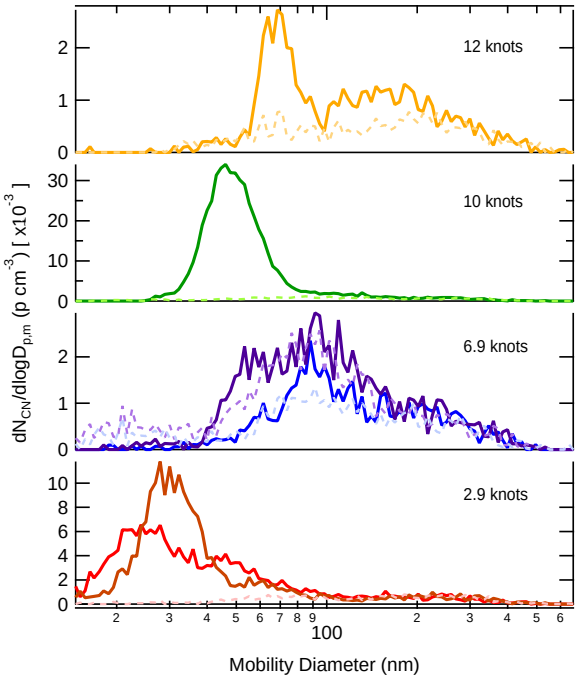

Fig. 3. Measured number-weighted particle mobility size distributions during plume intercepts at different vessel speeds. The solid lines indicate the distributions measured in the plumes while the dashed lines indicate distributions measured adjacent to the plumes and represent approximate background size distributions. The ability to distinguish plume distributions from background is not always apparent due to limited (random) overlap of the SMPS scanning cycle with the plume occurrence. However, for the 2.9, 10.2 and 12 knot intercepts a mode due to plume particles is clear.

ACPD
13, 24635–24674, 2013

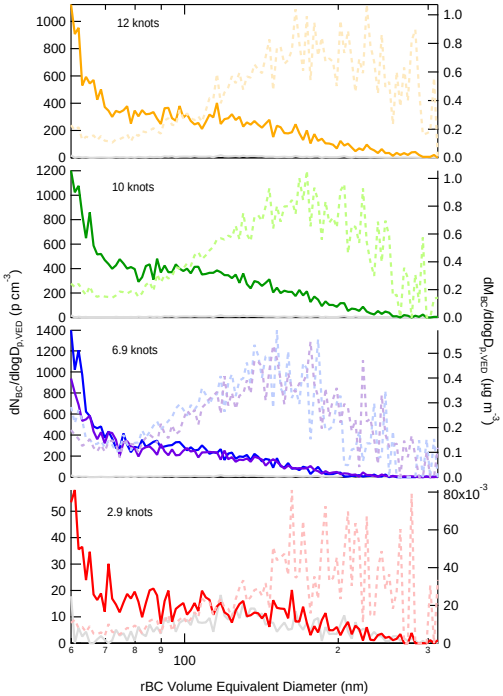

Fig. 4. Number-weighted (left axis and solid lines) and mass weighted (right axis and dashed lines) size distributions for the rBC component of particles for each plume intercept, averaged over the entire plume. The number-weighted distributions for background (outside of plume) particles are shown as the grey traces in all panels. For all but the 2.9 knots plume the observed size distribution is well above the background. The speed of the R/V *Miller Freeman* corresponding to each plume is indicated on each panel.

ACPD
13, 24635–24674, 2013

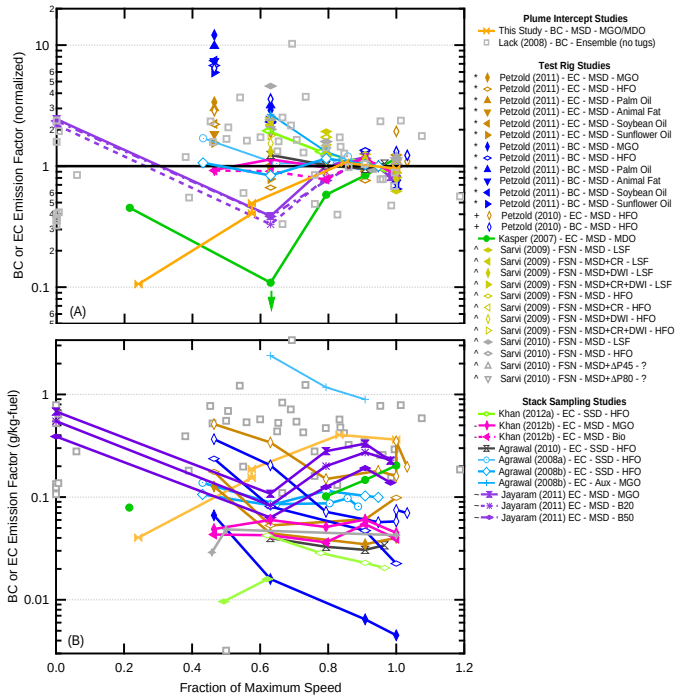

Fig. 5. Emissions factors (in g per kg-fuel) for black carbon (BC), elemental carbon (EC) or the "filter smoke number" (FSN) as a function of the vessel speed ratio for multiple studies **(A)** normalized to 85 % load and **(B)** as absolute values. The speed ratio is the ratio between the operating speed and the maximum ship speed, and for the test rig and stack sampling studies was estimated from the reported engine load using the propeller law. The legend groups the studies by measurement methodology: plume intercept, test rig and stack sampling. The symbols in the legend indicate which studies were performed on the same engine or ship. The legend names indicate the study, measured parameter (BC, EC or FSN), engine type (MSD or SSD) and fuel type (HFO or low sulfur, including biofuels, MDO and MGO). For the Sarvi studies, the additional information given after the engine type indicates a variation in the engine operation over the base case and includes use of a common rail injection system (CR), direct water injection (DWI), or variation in the fuel nozzle open pressure (ΔP). The downward green arrow indicates that the actual EF reported for this point was actually zero.

ACPD
13, 24635–24674, 2013

A case study into the measurement of ship emissions

C. D. Cappa et al.

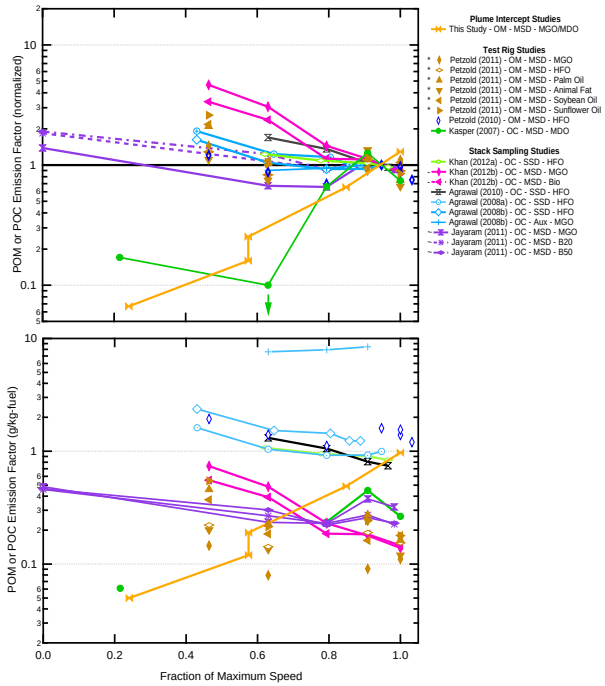

Fig. 6. Emissions factors (in g per kg-fuel) for primary organic matter (POM) or primary organic carbon (POC) as a function of the vessel speed ratio for multiple studies **(A)** normalized to 85 % load and **(B)** as absolute values. The speed ratio is the ratio between the operating speed and the maximum ship speed, and for the test rig and stack sampling studies was estimated from the reported engine load using the propeller law. The symbols in the legend indicate which studies were performed on the same engine or ship. The legend names indicate the study, reported parameter (POM or POC), engine type (MSD or SSD) and fuel type (HFO or low sulfur, including biofuels, MDO and MGO). The downward green arrow indicates that the actual EF reported for this point was actually zero.

ACPD
13, 24635–24674, 2013

A case study into the measurement of ship emissions

C. D. Cappa et al.

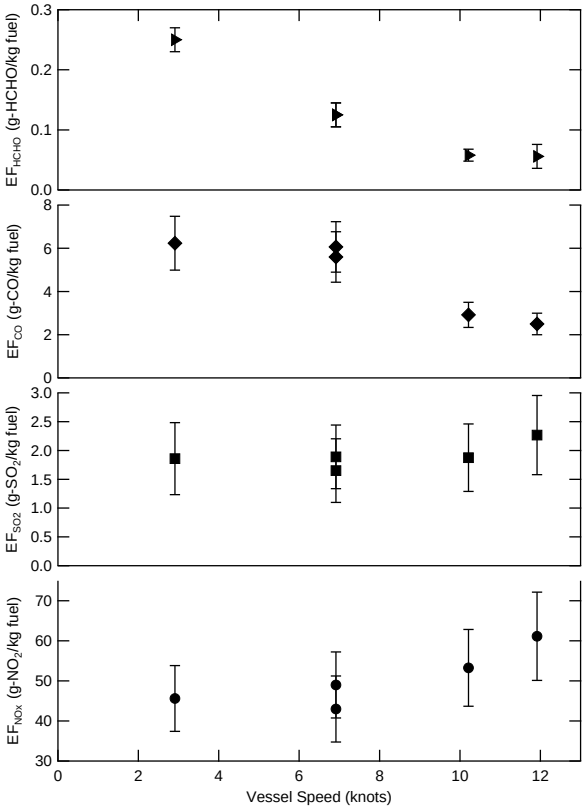

Fig. 7. Measured emissions factors, in g-X per kg-fuel for (top to bottom) HCHO, CO, SO_2 and NO_x (as NO_2) as a function of vessel speed.

ACPD
13, 24635–24674, 2013